

# Switchable beam steering with zenithal bistable liquid-crystal blazed gratings

Dimitrios C. Zografopoulos<sup>1,\*</sup> and Emmanouil E. Kriezis<sup>2</sup>

<sup>1</sup>*Consiglio Nazionale delle Ricerche, Istituto per la Microelettronica e Microsistemi, Roma 00133, Italy*

<sup>2</sup>*Department of Electrical and Computer Engineering,  
Aristotle University of Thessaloniki, Thessaloniki GR-54124, Greece*

compiled: September 1, 2014

**Switchable** beam steerers based on zenithal bistable liquid crystal gratings are designed and theoretically investigated. The nematic orientation profiles and the optical transmittance properties of the gratings are rigorously calculated, respectively, via a tensorial formulation of the Landau-de Gennes theory and the full-wave finite-element-method. By proper design of the grating geometry, beam steering with high diffraction efficiency is demonstrated between the two stable liquid crystal states. The tolerance of the device performance with respect to material parameters is assessed, evidencing spectral operation windows of more than 50 nm in the visible for a beam steering efficiency higher than 90%.

OCIS codes: 160.3710, 230.1950, 230.1360, 050.1755, 230.3720

<http://dx.doi.org/10.1364/XX.99.099999>

Nematic liquid crystals (LC) are anisotropic organic materials whose properties can be dynamically controlled via the application of external fields. This tunability, along with their large inherent optical anisotropy, has led to their integration in a large number of switchable devices for optics and photonics, ranging from displays to tunable waveguides, filters, and light beam control elements [1–6]. One major advantage of electro-optical LC-based devices is their very low power requirements, associated to the low-frequency electric field needed to keep the LC molecules in the switched state. Moving even further, it has been demonstrated that in certain geometries and under specific boundary conditions, nematic materials show bistable behaviour, *i.e.* there are two equilibrium stable states corresponding to different molecular orientation profiles. Such devices feature *zero* idle power consumption, since control pulses are required only when switching between the two states.

Among the various LC bistable structures thus far proposed, the zenithal bistable device (ZBD) has been proven as the most promising candidate, leading to the development of low-cost passively addressed displays for image storing with high mechanical strength and no image sticking [7]. In this geometry, the LC is confined between two surfaces treated to provide homeotropic anchoring for the LC molecules, one of which exhibits a grating structure, *e.g.* sinusoidal [8–10] or triangular [11]. In this letter, we extend the applicability of

ZBDs in the field of optical beam manipulation, by demonstrating efficient beam steering in optimally designed bistable LC blazed gratings. Compared to other types of LC-tunable optical gratings, the proposed ZBD beam steerers feature zero idle and very low switching power consumption, and ease of fabrication and integration by leveraging on the mature LC display technology. Moreover, they eliminate the need for complicated alignment patterns and/or external masks as in switchable photoalignment LC gratings [4], or high power control beams in azo-dye [5] or nonlinear-LC [6] all-optically controlled devices. The layout of the structure is presented in Fig. 1. The grating is characterized by its pitch  $p_0$ , and the width  $w_0$ , height  $a_0$ , and blazing parameter  $w_1$  of the triangular elements. The LC cell thickness is  $h_0 = 10 \mu\text{m}$  and is infiltrated with the well-known nematic mixture E7. The substrate and the grating are made of a polymer material with refractive index  $n_g$ .

Zenithal bistable LC gratings exhibit two stable states that correspond to a high-tilt, vertical aligned nematic (VAN) and a low-tilt, hybrid aligned nematic (HAN) configuration. In order to investigate the LC orientational properties of the proposed blazed gratings, we employ the  $\mathbf{Q}$  tensor formalism [12], which is capable of capturing the defect singularities and nematic order parameter variations in ZBD structures. In the most general case of biaxial solutions, the symmetric and traceless  $\mathbf{Q}$  matrix is expressed as  $\mathbf{Q} = S_1 (\mathbf{n} \otimes \mathbf{n}) + S_2 (\mathbf{m} \otimes \mathbf{m}) - 1/3 (S_1 + S_2) \mathbf{I}$ , where  $\mathbf{I}$  is the unitary matrix and  $\mathbf{n}$ ,  $\mathbf{m}$ , and  $\mathbf{n} \times \mathbf{m}$  are its eigenvectors with corresponding eigenvalues  $(2S_1 - S_2)/3$ ,  $(2S_2 - S_1)/3$ , and  $-(S_1 + S_2)/3$ . The total energy in the LC bulk is composed via three contri-

---

\* Corresponding author: dimitrios.zografopoulos@artov.imm.cnr.it

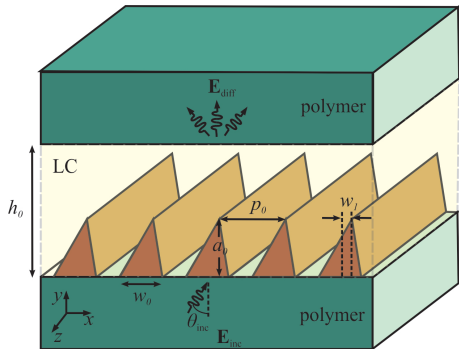


Fig. 1. Schematic layout and parameter definition of the proposed zenithal bistable liquid-crystal blazed grating.

butions expressed by the thermotropic, elastic, and electromagnetic energy density functions. Following the definitions as in [12], the thermotropic coefficients are equal to  $a = -0.3 \times 10^5 \text{ J/m}^3$ ,  $b = -1.5 \times 10^5 \text{ J/m}^3$ , and  $c = 2.5 \times 10^5 \text{ J/m}^3$  [13], leading to an equilibrium order parameter equal to  $S_{\text{eq}} = 0.6$ . The elastic coefficients used in the model are  $L_1 = (K_{33} - K_{11} + 3K_{22}) / (6S_{\text{eq}}^2)$ ,  $L_2 = (K_{11} - K_{22}) / S_{\text{eq}}^2$ , and  $L_6 = (K_{33} - K_{11}) / (2S_{\text{eq}}^3)$ , where  $K_{ii}$  are the corresponding Frank elastic constants, which for E7 are equal to  $K_{11} = 10.3 \text{ pN}$ ,  $K_{22} = 7.4 \text{ pN}$ , and  $K_{33} = 16.48 \text{ pN}$  [14]. The electrostatic energy density stems mainly from a dielectric component, where the relative permittivity tensor is given by  $\tilde{\epsilon}_r = \Delta\epsilon^* \mathbf{Q} + \bar{\epsilon} \mathbf{I}$ ,  $\Delta\epsilon^* = (\epsilon_{\parallel} - \epsilon_{\perp}) / S_{\text{eq}}$  being the scaled dielectric anisotropy and  $\bar{\epsilon} = (\epsilon_{\parallel} + 2\epsilon_{\perp}) / 3$ . The relative LC permittivities are equal to  $\epsilon_{\parallel} = 18.6$  and  $\epsilon_{\perp} = 5.31$  [14]. In addition, we have included the flexoelectric effect as in [13], described by two terms proportional to the coefficients  $p_1 = (e_{11} + e_{33}) / (2S_{\text{eq}})$  and  $p_2 = (e_{11} - e_{33}) / (2S_{\text{eq}}^2)$ , where the classical flexoelectric polarization coefficients  $e_{11}$  and  $e_{33}$  are equal to 15 and 10 pC/m, respectively [15].

Figure 2 shows the profiles of the  $q_1$  tensor element and the nematic order parameter  $S$  for the two states of the ZBD grating for the following set of geometrical parameters:  $p_0 = 1.6 \text{ }\mu\text{m}$ ,  $a_0 = 5.54 \text{ }\mu\text{m}$ ,  $w_0 = 1.26 \text{ }\mu\text{m}$ ,  $w_1 = 0.65 \text{ }\mu\text{m}$ . The reduction of the order parameter at the peak and bottom sides of the grating with respect to the equilibrium value  $S_{\text{eq}} = 0.6$  indicates the presence of point singularities. High (low) values of  $q_1$  correspond to LC molecular alignment parallel (perpendicular) to the direction of periodicity. In the VAN state the nematic orientation is perpendicular except for the region in the vicinity of the grating inclined surfaces where the homeotropic anchoring is imposed. The HAN state is characterized by an almost parallel alignment in the grating region, whereas the LC molecules progressively tilt towards the top surface of the LC cell.

The properties of the HAN state form the basis for the design of the ZBD diffractive element at the target wavelength of  $\lambda_0 = 633 \text{ nm}$ . First, a polymer material is selected such that the condition  $n_g = n_e$  is met, where  $n_e$

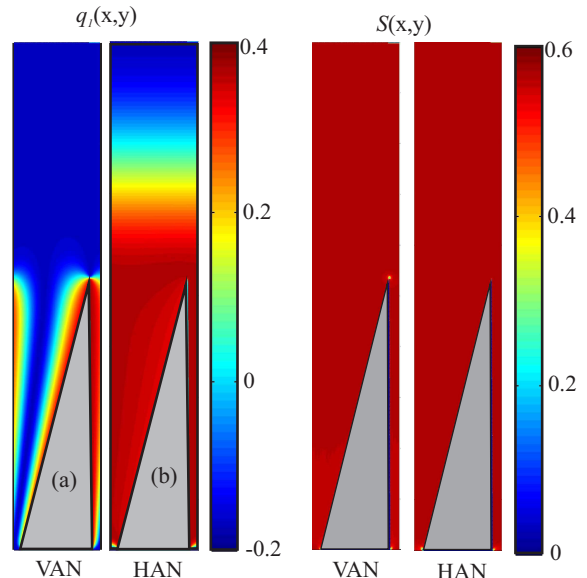


Fig. 2. Profiles of the  $q_1$  tensor element and the nematic order parameter for the two stable states of the LC-grating.

is the extraordinary LC index. The ordinary  $n_o$  and extraordinary indices for E7 at  $\lambda_0$  are equal to  $n_o = 1.519$  and  $n_e = 1.73$  [16]. This condition leads to minimal diffraction in the HAN state for a  $x$ -polarized normally impinging plane wave, which senses a refractive index equal to the matched value  $n_g = n_e$  around the grating, and thus minimal index modulation. The investigation of the diffractive properties of the ZBD grating is conducted by employing the finite-element-method in the commercial tool COMSOL Multiphysics™ (v4.4). The transmitted field  $\mathbf{E}^t$  is calculated at a constant  $y = y_0$  plane in the superstratum and its  $x$ -component is expanded in a 1-D Floquet series, according to

$$E_x^t(x, y = y_0) = \sum_m E_{x,m}^t e^{-j\beta_m y}, \quad (1)$$

where  $\beta_m = \beta_0 + 2\pi m / p_0$ ,  $\beta_0 = (2\pi n_g / \lambda_0) \sin(\theta_{\text{inc}})$  being the polymer wavenumber projection in the direction of periodicity ( $x$ -axis) and  $\theta_{\text{inc}}$  the angle of incidence as in Fig. 1. The amplitudes  $E_{x,m}^t$  are obtained from orthogonality considerations with an integration over a grating period,

$$E_{x,m}^t = \frac{1}{p_0} \int_{y=y_0} E_x^t(x, y_0) e^{j\beta_m y} dx. \quad (2)$$

Finally, the total diffraction efficiency (DE) for each propagating diffraction order is calculated by

$$\text{DE}_m = \frac{P_m}{P^i} = \frac{|E_{x,m}^t|^2}{|E_x^i|^2 |\cos \theta_m|}, \quad (3)$$

where  $P^i$ ,  $E_x^i$  are the power and amplitude of the inci-

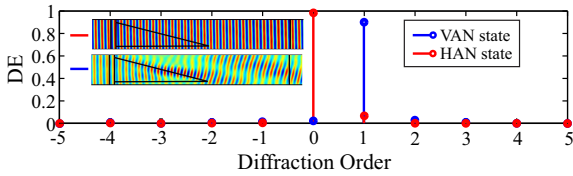


Fig. 3. Efficiencies of the diffraction modes for  $m = -5, \dots, 5$  for the proposed ZBD beam steerer. Inset shows the profile of the  $E_x$  component for both states. All geometrical parameters are as in Fig. 2.

dent electric field, respectively, and  $\cos \theta_m$  is given by

$$\cos \theta_m = \frac{\sqrt{(k_0 n_g)^2 - \beta_m^2}}{k_0 n_g}, \quad (4)$$

where  $\theta_m$  is the deflection angle for mode  $m$  and  $k_0 = 2\pi/\lambda_0$  is the free space wavenumber.

The index matching condition minimizes light diffraction for the HAN configuration. In the VAN state, the grating's diffractive properties depend on the structure's geometry. The next step is to let the grating parameters, as defined in Fig. 1, vary within a relevant parameter space and implement a Nelder-Mead optimization algorithm, aiming to identify the geometry that maximizes the DE of the  $m = 1$  mode. The resulting set of parameters is the one used for the LC profiles in Fig. 2. The diffractive properties of the LC grating for the optimum design are summarized in Fig. 3, which plots the efficiencies for the  $m = -5, \dots, 5$  diffraction modes calculated for both LC states. The DE of the  $m = 0$  and  $m = 1$  modes for the HAN and VAN states, respectively, is 99% and 91%, indicating efficient beam steering by switching between the two states. The DE of all other undesired modes are suppressed below 4%, the largest being that of the  $m = 2$  mode in the VAN state.

The angular dependence of the grating's properties is investigated in Fig. 4. Owing to the matching condition, the HAN state remains practically non-diffracting for an angle of incidence  $\theta_{\text{inc}}$  varying from  $-10$  to  $10^\circ$ . The VAN diffracting state shows an angular bandwidth of  $2^\circ$ , defined as the angular range where the DE remains above 90% of its maximum value. For diverging angles of incidence the optical power is transferred to other diffraction modes. For  $\theta_{\text{inc}} = 5.8^\circ$  the VAN state also becomes non diffracting, as more than 90% of the total transmitted power stays in the  $m = 0$  mode. On the contrary, when  $\theta_{\text{inc}} = -6.4^\circ$  it is the DE of the  $m = 2$  mode that is maximized, indicating an alternative possibility for beam steering through the ZBD grating. It is remarked that owing to the bistable operation of the ZBD grating, there is no possibility for continuous tuning of the deflection angle  $\theta_m$ , which is fixed once the grating geometry is optimized at a given wavelength.

The proposed design optimizes the grating's performance at the target wavelength by requiring that the matching condition  $n_g = n_e$  is met. The same design

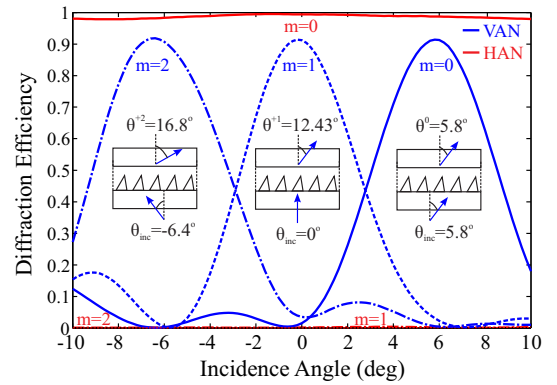


Fig. 4. Dependence of the diffraction efficiency for the  $m = 0$  and  $m = 1$  modes of the HAN and VAN states, respectively, on the angle of incidence. All parameters as in Fig. 2.

procedure can be applied for any wavelength, meaning that such beam steering switches can also be extended in the near infrared spectrum. In general, there is an abundance of nematic materials synthesized for LC-based applications sharing the same range of extraordinary refractive indices with photo-patternable polymers [17]. In order to estimate the sensitivity of the matching condition, the beam steerer's efficiency with respect to the matching condition, as well as the operation wavelength, is investigated in Fig. 5. The DE of the  $m = 0$  HAN and the  $m = 1$  VAN state is calculated in the wavelength range from 550 to 700 nm and for a variation of the polymer index from 1.7 to 1.76. The LC material stays fixed, namely E7, and its material dispersion is included via a Cauchy model [16]. It is demonstrated that there are large operation windows both in terms of the polymer index and operation wavelength without significant deterioration of the steerer's performance. This behaviour is attributed to the fact that the grating's optical diffractive properties are not the result of a resonant phenomenon. By setting as a performance criterion a DE higher than 90% for both states, the bandwidth at the index matching condition is  $\Delta\lambda = 64$  nm, while the permitted refractive index interval at  $\lambda_0 = 633$  nm is  $\Delta n_g = 0.025$ . This implies that the design is robust to small variations of its optimal parameters.

**Switchable** beam steering in the proposed ZBD gratings can be achieved by alternating between the two LC states corresponding to local minima of the total LC energy. In order to surpass the energy barrier separating the two states, a voltage is applied across the LC cell, by means of a pair of uniform planar ITO electrodes, as in ZBD technology for display applications. Depending on the amplitude, duration and polarity, the control pulse can cause defect nucleation or annihilation, mediating the transition between the VAN and HAN states. The procedure is governed by two effects, the dielectric and flexoelectric coupling of the nematic orientation with the applied electric field, both of which can be exploited.

Flexoelectric switching stems from the large distur-

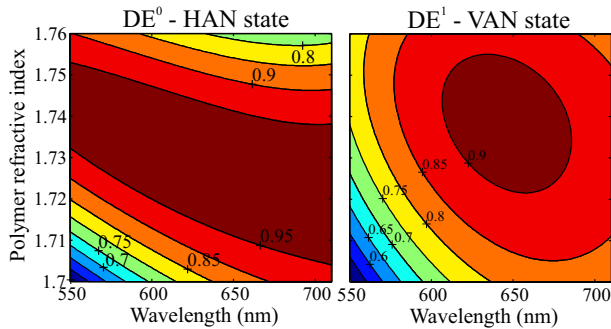


Fig. 5. Dependence of the diffraction efficiency for the  $m = 0$  and  $m = 1$  modes of the HAN and VAN states, respectively, on the operation wavelength and the polymer index.

tion of the director field near the grating surface, and the torque generated by the applied field, which causes defect annihilation or nucleation depending on the field polarity [13, 18]. The switching threshold, expressed in terms of the product  $\tau V_0$ , where  $\tau$  and  $V_0$  are the voltage pulse duration and amplitude, respectively [19–21], can be lowered [20, 22] to sub-millisecond times with voltages below 10 V, when using optimized LC mixtures, which provide high  $\Delta\epsilon$  and low viscosities [23]. Assuming values of this order of magnitude, the energy to switch a ZBD beam steerer of active surface  $S = 1 \text{ cm}^2$ , estimated by  $E_s \simeq CV_0^2 f \tau$ , where  $C$  the maximum capacitance of the LC cell, approximated as  $C \simeq \epsilon_0 \epsilon_e S / h_0$  and  $f = 1 \text{ KHz}$  the control frequency, is less than  $1 \mu\text{J}$ . It is stressed that the device needs to consume energy only when the switching pulse is applied and not in idle operation in either of the two states. Another possibility for switching is the use of dual-frequency LC materials, via the reversal of the sign of  $\Delta\epsilon$  by means of adjusting the frequency of the control voltage, which is a standard option for the control of LC-tunable devices including bistable LC cells and gratings [24]. The technique relies purely on the dielectric effect, thus avoiding the complications of ionic migration that can occur in flexoelectrically driven switching [22].

In conclusion, we have presented the design of a LC-tunable beam steerer based on blazed zenithal bistable gratings. The grating’s design is optimized such that by switching between the two LC states, it alternates between non diffractive operation and efficient beam steering towards the first order diffraction mode. The grating’s angular and spectral bandwidth has been investigated, showing that efficient steering is provided in windows of several tens of nanometers, with significant tolerance on the design matching condition in terms of material selection. The device consumes zero idle and very low switching power consumption, owing to capacitive operation in the electro-optic addressing of the LC cell. Fabrication of the device and integration of the switching mechanism can leverage the already developed technology in the field of zenithal bistable displays. The proposed gratings may find applications as ultra-low-

power beam-control components in consumer electronics devices, such as holographic switches, projection systems, or CD/DVD systems.

This work was supported by the Italian Ministry of Foreign Affairs, Directorate General for the Country Promotion and by the European Union and Greek national funds through the National Strategic Reference Framework, Research Funding Program THALES (Project ANEMOS). The authors would like to thank Dr. Nigel Mottram for helpful discussions.

## References

- [1] D. C. Zografopoulos, R. Asquini, E. E. Kriezis, A. d’Alessandro, and R. Beccherelli, *Lab Chip* **12**, 3598 (2012).
- [2] J. Beeckman, K. Neyts, P. J. M. Vanbrabant, *Opt. Eng.* **50**, 081202 (2011).
- [3] C. V. Brown, E. E. Kriezis, and S. J. Elston, *J. Appl. Phys.* **91**, 3495 (2002).
- [4] J. Sun, A. K. Srivastava, L. Wang, V. G. Chigrinov, and H. S. Kwok, *Opt. Lett.* **38**, 2342 (2013).
- [5] L. De Sio, S. Serak, N. Tabiryan, and T. Bunning, *J. Mater. Chem. C* **2**, 2532 (2014).
- [6] N. V. Tabiryan and S. R. Nersisyan, *Appl. Phys. Lett.* **84**, 5145 (2004).
- [7] C. Jones, “Bistable Liquid Crystal Devices”, (Springer, 2012) Chap. 7.3.5 in *Handbook of Visual Display Technology*, 1507–1543.
- [8] G. P. Bryan-Brown, C. V. Brown, and J. C. Jones, US Patent No. US6249332 (1995).
- [9] E. G. Edwards, C. V. Brown, E. E. Kriezis, S. J. Elston, S. C. Kitson, and C. J. P. Newton, *Mol. Cryst. Liq. Cryst.* **410**, 401 (2004).
- [10] T. J. Spencer, C. M. Care, R. M. Amos, and J. C. Jones, *Phys. Rev. E* **82**, 021702 (2010).
- [11] J. C. Jones, *Proceedings of the SID* **51.2**, 1626 (2006).
- [12] G. Lombardo, H. Ayeb, R. Barberi, *Phys. Rev. E* **77**, 051708 (2008).
- [13] L. A. Parry-Jones, R. B. Meyer, and S. J. Elston, *J. Appl. Phys.* **106**, 014510 (2009).
- [14] J. F. Strömer, E. P. Raynes, and C. V. Brown, *Appl. Phys. Lett.* **88**, 051915 (2006).
- [15] Á. Buka and N. Éber, eds., *Flexoelectricity in liquid crystals* (Imperial College Press, 2013).
- [16] J. Li, C.-H. Wen, S. Gauza, R. Lu, and S.-T. Wu, *J. Display Technol.* **1**, 51 (2005).
- [17] C. Lü, C. Guan, Y. Liu, Y. Cheng, and B. Yang, *Chem. Mater.* **17**, 2448 (2005).
- [18] L. A. Parry-Jones and S. J. Elston, *J. Appl. Phys.* **97**, 093515 (2005).
- [19] A. J. Davidson and N. J. Mottram, *Phys. Rev. E* **65**, 051710 (2002).
- [20] C. V. Brown, L. Parry-Jones, S. J. Elston, and S. J. Wilkins, *Mol. Cryst. Liq. Cryst.* **410**, 417 (2004).
- [21] J. C. Jones and R. M. Amos, *Mol. Cryst. Liq. Cryst.* **543**, 57 (2011).
- [22] J. C. Jones, S. Beldon, P. Brett, M. Francis, and M. Goulding, *Proceedings of the SID* **26.3**, 954 (2003).
- [23] M. Francis, M. J. Goulding, J. C. Jones, S. Beldon, US Patent No. 2006/0115603 A1 (2006).
- [24] S. P. Palto and M. I. Barnik, *J. Exp. Theor. Phys.* **102**, 998 (2006).

## Informational Page

Full versions of citations.

## References

- [1] D. C. Zografopoulos, R. Asquini, E. E. Kriezis, A. d'Alessandro, and R. Beccherelli, "Guided-wave liquid-crystal photonics," *Lab Chip* **12**, 3598 (2012).
- [2] J. Beeckman, K. Neyts, P. J. M. Vanbrabant, "Liquid-crystal photonic applications," *Opt. Eng.* **50**, 081202 (2011).
- [3] C. V. Brown, E. E. Kriezis, and S. J. Elston, "Optical diffraction from a liquid crystal phase grating," *J. Appl. Phys.* **91**, 3495 (2002).
- [4] J. Sun, A. K. Srivastava, L. Wang, V. G. Chigrinov, and H. S. Kwok, "Optically tunable and rewritable diffraction grating with photoaligned liquid crystals," *Opt. Lett.* **38**, 2342 (2013).
- [5] L. De Sio, S. Serak, N. Tabiryan, and T. Bunning, "Nanosecond switching of photo-responsive liquid crystal diffraction gratings," *J. Mater. Chem. C* **2**, 2532 (2014).
- [6] N. V. Tabiryan and S. R. Nersisyan, "Large-angle beam steering using all-optical liquid crystal spatial light modulators," *Appl. Phys. Lett.* **84**, 5145 (2004).
- [7] C. Jones, "Bistable Liquid Crystal Devices", (Springer, 2012) Chap. 7.3.5 in *Handbook of Visual Display Technology*, 1507–1543.
- [8] G. P. Bryan-Brown, C. V. Brown, and J. C. Jones, "Bistable nematic liquid crystal device," US Patent No. US6249332 (1995).
- [9] E. G. Edwards, C. V. Brown, E. E. Kriezis, S. J. Elston, S. C. Kitson, and C. J. P. Newton, "Diffraction from the two stable states in a nematic liquid crystal cell containing a mono-grating with homeotropic director alignment," *Mol. Cryst. Liq. Cryst.* **410**, 401 (2004).
- [10] T. J. Spencer, C. M. Care, R. M. Amos, and J. C. Jones, "Zenithal bistable device: Comparison of modeling and experiment," *Phys. Rev. E* **82**, 021702 (2010).
- [11] J. C. Jones, "Novel geometries of the zenithal bistable device," *Proceedings of the SID* **51.2**, 1626 (2006).
- [12] G. Lombardo, H. Ayeb, R. Barberi, "Dynamical numerical model for nematic order reconstruction," *Phys. Rev. E* **77**, 051708 (2008).
- [13] L. A. Parry-Jones, R. B. Meyer, and S. J. Elston, "Mechanisms of flexoelectric switching in a zenithally bistable nematic device," *J. Appl. Phys.* **106**, 014510 (2009).
- [14] J. F. Strömer, E. P. Raynes, and C. V. Brown, "Study of elastic constant ratios in nematic liquid crystals," *Appl. Phys. Lett.* **88**, 051915 (2006).
- [15] Á. Buka and N. Éber, eds., *Flexoelectricity in liquid crystals* (Imperial College Press, 2013).
- [16] J. Li, C.-H. Wen, S. Gauza, R. Lu, and S.-T. Wu, "Refractive indices of liquid crystals for display applications," *J. Display Technol.* **1**, 51 (2005).
- [17] C. Lü, C. Guan, Y. Liu, Y. Cheng, and B. Yang, "PbS/Polymer nanocomposite optical materials with high refractive index," *Chem. Mater.* **17**, 2448 (2005).
- [18] L. A. Parry-Jones and S. J. Elston, *J. Appl. Phys.* "Flexoelectric switching in a zenithally bistable nematic device," **97**, 093515 (2005).
- [19] A. J. Davidson and N. J. Mottram, "Flexoelectric switching in a bistable nematic device," *Phys. Rev. E* **65**, 051710 (2002).
- [20] C. V. Brown, L. Parry-Jones, S. J. Elston, and S. J. Wilkins, "Comparison of theoretical and experimental switching curves for a zenithally bistable nematic liquid crystal device," *Mol. Cryst. Liq. Cryst.* **410**, 417 (2004).
- [21] J. C. Jones and R. M. Amos, "Relating display performance and grating structure of a zenithal bistable device," *Mol. Cryst. Liq. Cryst.* **543**, 57 (2011).
- [22] J. C. Jones, S. Beldon, P. Brett, M. Francis, and M. Goulding, "Low voltage zenithal bistable devices with wide operating windows," *Proceedings of the SID* **26.3**, 954 (2003).
- [23] M. Francis, M. J. Goulding, J. C. Jones, S. Beldon, "Fast switching liquid crystal compositions for use in bistable liquid crystal devices," US Patent No. 2006/0115603 A1 (2006).
- [24] S. P. Palto and M. I. Barnik, "Bistable switching in dual-frequency liquid crystals," *J. Exp. Theor. Phys.* **102**, 998 (2006).